Extreme events and single-pulse spatial patterns observed in a self-pulsing all-solid-state laser

Carlos Bonazzola,[1] Alejandro Hnilo,[1,*] Marcelo Kovalsky,[1] and Jorge Tredicce[2]

[1]*Centro de Investigaciones en Láseres y Aplicaciones (CEILAP), Instituto de Investigaciones Científicas y Técnicas para la Defensa (CITEDEF), Consejo Nacional de Investigaciones Científicas y Tecnológicas (CONICET), J. B. de La Salle 4397, (1603) Villa Martelli, Argentina*

[2]*Departamento de Física, Facultad de Ciencias Exactas y Naturales, Universidad de Buenos Aires, Intendente Güiraldes 2160, Ciudad Autónoma de Buenos Aires, Argentina and Université de la Nouvelle Calédonie, ISEA, Boîte Postale R4, Noumea, Nouvelle Calédonie, France*

(Received 30 August 2017; revised manuscript received 6 March 2018; published 26 March 2018)

The passively Q-switched, self-pulsing all-solid-state laser is a device of widespread use in many applications. Depending on the condition of saturation of the absorber, which is easy to adjust, different dynamical regimes are observed: continuous-wave emission, stable oscillations, period doubling bifurcations, chaos, and, within some chaotic regimes, extreme events (EEs) in the form of pulses of extraordinary intensity. These pulses are sometimes called "dissipative optical rogue waves." The mechanism of their formation in this laser is unknown. Previous observations suggest they are caused by the interaction of a few transverse modes. Here we report a direct observation of the pulse-to-pulse evolution of the transverse pattern. In the periodical regimes, sequences of intensities are correlated with sequences of patterns. In the chaotic ones, a few different patterns alternate, and the EEs are related with even fewer ones. In addition, the series of patterns and the pulse intensities before and after an EE are markedly repetitive. These observations demonstrate that EEs follow a deterministic evolution, and that they can appear even in a system with few interacting modes. This information plays a crucial role for the development of a mathematical description of EEs in this laser. This would allow managing the formation of EE through control of chaos, which is of both academic and practical interest (laser rangefinder).

DOI: 10.1103/PhysRevE.97.032215

I. INTRODUCTION

Waves of very high amplitude randomly appearing in deep ocean waters are important phenomena, which have been named "freak" or "rogue" waves [1]. In the last decade, scientific interest has increased on analogous rare or extreme events (EEs) of large amplitude observed in other areas. In optics, optical rogue waves were first observed in the intensity fluctuations of light at the edge of the spectrum produced by ultrashort laser pulse pumped optical fibers in the threshold of supercontinuum generation [2,3]. Conditions for their formation were later studied in experiments using optical fibers [4]. Optical EEs were also observed in a Vertical-Cavity Surface-Emitting Laser (VCSEL) with an injected signal [5], in fiber lasers [6–9], in Kerr-lens mode locked Ti:sapphire lasers [10] and, that which is our scope here, in self-pulsing (or passive Q-switch) high Fresnel number all-solid-state lasers with a "slow" saturable absorber (SA) [11]. EEs have also been studied in VCSELS with a (one-dimensional) transversally extended cavity with SA, which is a system rather similar to ours, although with a faster dynamics [12,13]. It is worth mentioning that chaotic intermittency seems to be a feature common to both systems. Reference [14] is a review on optical rogue waves.

The all-solid-state passively Q-switched laser is a small, robust, efficient and inexpensive device. It is used in many applications, from sparks in experimental inner-combustion engines to rangefinders and target illuminators. EEs spontaneously appear and are easily observed in the chaotic regime of this laser if the Fresnel number of the cavity is large. This condition is reached more easily than not, because the pump beam is, in general, difficult to focus, which naturally produces an active region (and hence, a limiting aperture) much broader than the cavity mode. A laser of this type working in the regime with EEs is therefore easy to build and robust to operate. Controlling the formation of EEs in this system is hence of practical interest. It would allow the generation, at selected times, of pulses of intensity two to three times higher than normally obtained from the same device, with no need to scale up the power supply and heat sink. This is especially useful if the laser is to be used, e.g., as the emitter in a rangefinder aboard a small, low cost unmanned flying vehicle, an application where weight is a crucial issue.

The system also has a broad academic interest. The equations of the single mode laser+SA are homologous to those of the Bénard-Rayleigh problem with a solute. The high Fresnel number laser with SA in the limit of small nonlinearity is described by a nonlinear Schrödinger equation, hence relating it directly with other systems where rogue phenomena have been observed. Yet, the precise mathematical framework to describe an EE in this laser is still to be determined. A key question is whether the number of modes playing a significant role in the dynamics is large or small. If it is large, the description involves a transversal Laplacian, as in the broad area VCSEL with SA [15]. This means a system of

*ahnilo@citedef.gob.ar

partial differential equations. If it is small instead, a simpler system of ordinary differential equations may suffice. Previous observations [11,16] suggest that the regimes with EE in this laser correspond to the second case. In order to confirm this hypothesis, it was proposed to observe the pulse-to-pulse evolution of the (complex) transverse pattern of the laser spot. This is difficult, because of the high repetition rate (tens of KHz) of the self-pulsing, and the intrinsic time instability of chaotic regimes.

In this paper we present the results of the observation of the pulse-to-pulse evolution of the transverse pattern of a self-pulsing laser. This is possible thanks to the use of an ultrafast camera [up to 6×10^4 frames per second (fps)] and two oscilloscope-to-camera matching software codes, which we develop for this specific purpose. These results demonstrate that EEs can appear even in a system with few interacting modes. Our observations guide the development of a mathematical description by outlining the key points to be reproduced. The description should be not only correct, but also as simple as possible, for our final goal is to manage the formation of EEs through control of chaos. As it is said, this is of both academic and practical interest.

Note that in most experimental work on nonlinear dynamics in optical systems the mathematical description of the problem is known. Here instead, we start from a real-world existing system (the all-solid-state laser+SA) where the phenomenon (the EE) appears spontaneously, and our goal is to find the appropriate (i.e., not only correct, but also as simple as possible) mathematical description in order to implement its practical application.

During the process of revision of this paper, questions were made about the number and role of longitudinal modes involved. Because of the cavity length and design, longitudinal and transversal modes (of the empty cavity) with different labels are closely spaced and mixed. They couple nonlinearly and bunch into "supermodes," which are characteristic of the homogeneous-inhomogeneous broadening of solid-state lasers [17]. Dynamics are then ruled by the interaction among supermodes (and the unobservable populations in the active medium and the absorber, of course). The supermodes, which are what we *observe*, not the (empty cavity) modes, are the elements necessary to develop a description.

At this stage of our research program, the questions are as follows: (i) Is the steady and complex transverse pattern observed with a standard (50 fps) camera the superposition of many different patterns, or is it a single pattern that repeats itself in every pulse in the chaotic series? (ii) In the case the patterns change from one pulse to the next, how many different patterns exist? (iii) Are the EEs associated with a single pattern? (iv) Is an EE due to the formation of a "hot spot" of higher intensity in the pattern or, instead, to a higher illumination of the whole pattern? (v) Are the EEs predictable? Specifically, do the patterns before and after an EE follow a particular sequence (as was observed in the pulse intensities [16]) or not?

II. EXPERIMENTAL SETUP

The setup is sketched in Fig. 1. The output of a 2-W (at 808 nm) continuous-wave laser diode is focused to a spot 0.8 mm diameter into a Nd : YVO_4 crystal, 1% doped with standard dichroic coating. The V-shaped laser cavity has a folding HR concave mirror and a plane output coupler. The operating wavelength of the laser is 1064 nm, linearly polarized. The mode size varies strongly between mirrors, with a waist near the output coupler. The cavity's Fresnel number is ≈10. A solid-state SA (Cr:YAG) is placed between the folding mirror and the output coupler at position X. Adjusting this position, the mode size at the SA changes and hence the condition of saturation. This is the main control parameter in this system. As it is varied different dynamical regimes appear, from stable Q switch to periodic bifurcations and chaotic regimes with and without EEs. The average output power is practically the same in all the regimes, about 300 mW for 1.8 W pump power. The pulse duration is ≈100 ns. This means a typical average peak power of 125 kW.

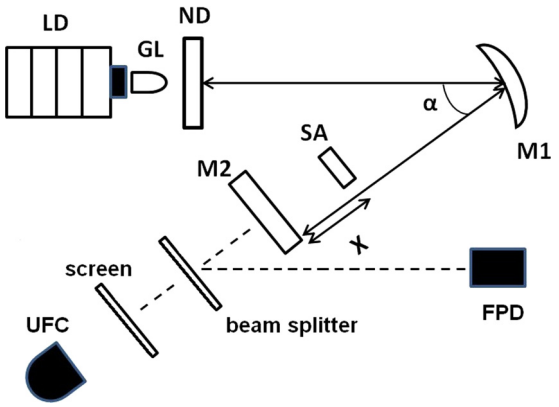

FIG. 1. Sketch of the setup. LD: pump laser diode, 2 W cw at 808 nm; GL: GRIN lens; ND: Nd : YVO_4 slab $3 \times 3 \times 1\,mm^3$ 1% doped; M1: folding mirror (HR, $R = 10\,cm$); M2: output mirror (reflectivity 98%, plane); SA: Cr:YAG crystal, transmission (unbleached) 90%; $\alpha = 20°$; distance ND − M1 = 13cm; M1 − M2 = 7 cm; the position X is adjusted to get different dynamical regimes; FPD: fast photodiode connected to a digital memory oscilloscope; UFC: ultrafast camera recording single pulse spot images; the screen is translucent. By unblocking the laser beam between M2 and the beam splitter, the camera and the oscilloscope, which are both set in the autotrigger mode, start recording at the same time. Yet, the intensities and images series rapidly get out of synchronism, so that a special software code had to be developed to determine what image corresponds to each pulse.

A beam splitter divides the laser output in two: One part is focused into a fast photodiode (100 ps rise time) connected to a digital storage oscilloscope (PicoScope 6403B: 350 MHz bandwidth, 5 GS/s, memory 1 GS); the other part is projected in a translucent screen and observed and recorded with an ultrafast camera (Photron Fastcam SA-3). The oscilloscope records the shape of the laser pulses, while the camera simultaneously records the transverse pattern of the laser spot. The synchronous start of both recordings is ensured by blocking (and then unblocking) the laser beam between the output mirror and the beam splitter (see Fig. 1), and by setting both the oscilloscope and the camera in "autotrigger" mode (see Supplemental Material [18]).

The spatial resolution of the camera decreases if the number of fps is increased. There is a discrete set of "fps × resolution" combinations available in the camera's software menu. In the

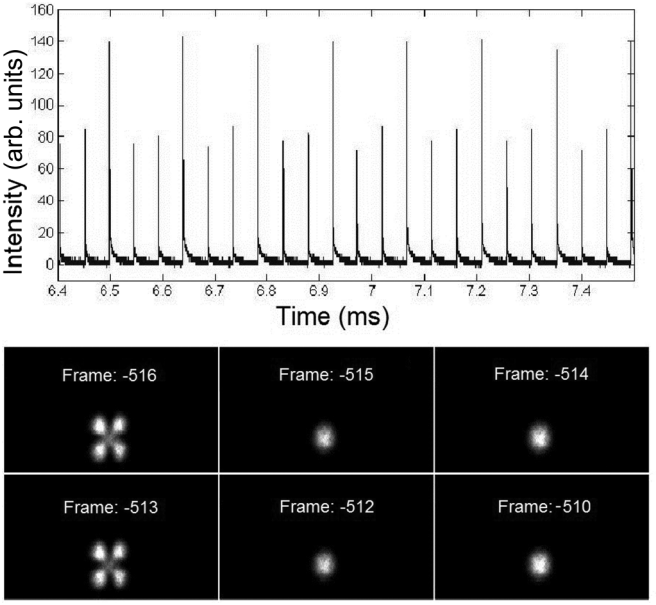

FIG. 2. Pulse intensity and corresponding patterns for a period-3 regime. Note the successive labels of the camera shots (from −516 to −510). As an illustration of a typical error, we show here a case where the camera fired between two successive pulses and is an empty image (frame −511, not shown).

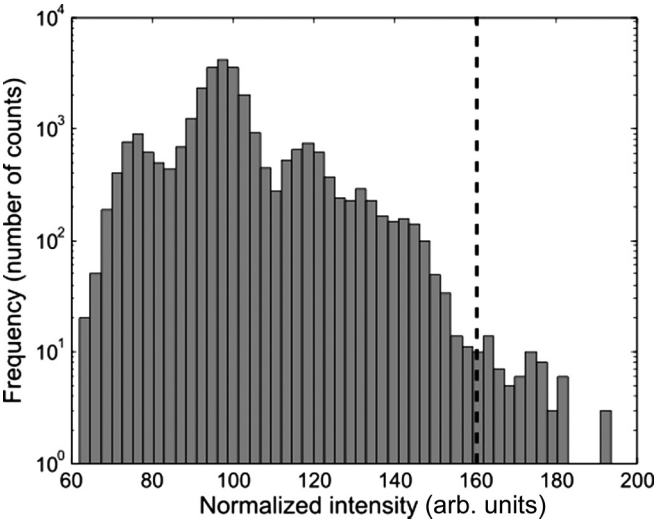

FIG. 3. Histogram of peak pulse intensities (run 2b9/29/16, 27779 pulses). The horizontal axis is normalized such that the average intensity = 100. The threshold value for EE is 161 (vertical line); there are 64 EE, $d_E = 8$, two positive Lyapunov exponents, and $K = 5.1$.

periodic regimes, the repetition rate of the laser does not fit exactly the values in this menu and, besides, there is a "blind time" after each camera shot. For these reasons, during a long run the patterns corresponding to some pulses are lost (an illustration of this problem is shown in Fig. 2). In the chaotic regimes the situation is even worse, for the pulse separation changes wildly. The camera may miss the patterns corresponding to some pulses, or it may record in the same frame the patterns corresponding to two successive pulses that are unusually close in time. Fortunately, if the fps of the camera and the average repetition rate of the laser roughly fit, and some special care is taken (see later) the number of pulses missed or jammed in a long series is found to be low. In all the runs discussed in this paper, the laser repetition rate is ≈ 24 KHz, the camera is set to 25000 fps, the resolution to 128 × 80 pixels, and the blind time to 1.32 μs. The acquisition time of each frame is thus 38.68 μs, much longer than the pulse duration. Hence, each image is the time-integrated transverse pattern of one pulse (rarely, two pulses).

Here is a brief note on the definition of the EE threshold value: It usually is (a) amplitude higher than twice the "significant wave height" or "significant intensity" $I_{1/3}$, which is the average calculated among the set of the one-third highest events in the series. Alternatively, (b) amplitude higher than 4 times the standard deviation. Here we use the definition (b). The kurtosis K is an additional measure of non-Gaussian feature; $K > 3$ means a distribution with a tail longer and higher than that of a Gaussian one.

III. OBSERVATIONS

A. An example: period three regime

Depending on the position X of the SA, different dynamical regimes are observed. The intensity output and the sequence of spatial patterns for a period-3 regime are displayed in Fig. 2. It is clearly seen that the periodic evolution of the pulse intensity corresponds to a periodic repetition of spatial patterns. The pulse with the highest intensity corresponds to a fourfold pattern (called E; see next section), while the two smaller ones correspond to TEM_{00} -like patterns (called A). The sequence repeats indefinitely.

B. Chaotic regime with EEs

Now we adjust the SA position so that the laser is in a chaotic regime with EEs. In what follows, for reasons of space, we discuss in detail the results for one particular run (internal identification: 2b9/29/16). It is representative of many other runs. If the average peak intensity is scaled to 100, the EE threshold in this run is 161 and 64 pulses are EEs (see Fig. 3). The kurtosis value is 5.1. The complete series has 27779 pulses (a sample zoom is shown in Fig. 4). It is analyzed with the TISEAN free software package [19,20]. The value of the dimension of embedding (d_E) is found by the decay of the fraction of false neighbors and is computed between 8 and 10. This determines the dimensionality of the dynamics. The sum of the Lyapunov exponents is negative, showing the system is dissipative. Two of them are positive, showing the regime is chaotic.

The time separation between pulses changes in an irregular way, so that the images corresponding to some pulses can be missed, or two get superimposed. Besides, there is a slight drift between the internal clocks of the oscilloscope and the camera. For these reasons, even if the number of missed or jammed images is small, the identification of the (camera) image that corresponds to an (oscilloscope) pulse is not immediate. We then develop a computer code that matches images and pulses. It is based on the correlation between two series: the integral below the pulse in the oscilloscope trace obtained for a test partition, and the integrated intensity in the camera image. Both series are proportional to the total energy of each pulse, so that

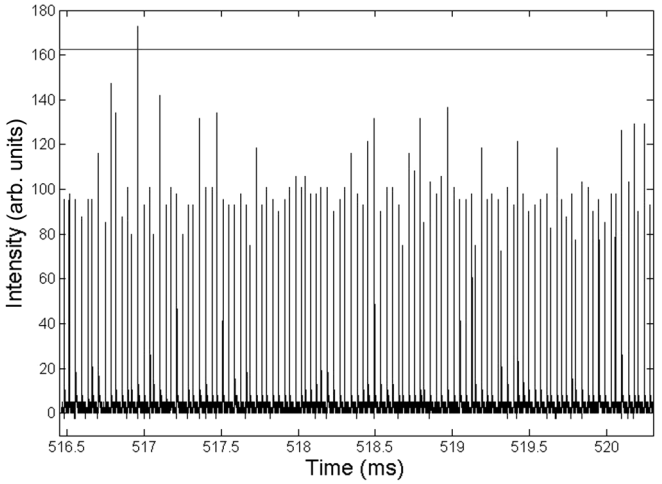

FIG. 4. Sample zoom of the oscilloscope trace for run 2b9/29/16. Note the EE just before time = 517 ms.

they are naturally correlated. The code adjusts the partition to maximize the correlation.

We then find that the correlation between pulses and images series decays with time. This is caused by a relative drift $\approx 10\ \mu$s/s between the clocks in the oscilloscope and the camera. This drift is corrected whenever the calculated correlation decays below a threshold. This code is useful to correlate any type of one-column series with a nonsynchronous series of images, provided that both have some magnitude in common (in our case, the pulse total energy) (see the Supplemental Material [18] for the details).

In the chaotic series we identify eight different types of patterns, that we name A–H (Fig. 5). The relative frequency of each pattern in the series is indicated, also the image observed with a standard camera (which is steady). Now we can answer question (i): The steady complex pattern observed at low time resolution is the superposition of hundreds of different patterns that alternate chaotically. We can also answer question (ii): There are few types of simple patterns. Besides, some of the less frequent patterns are probably the superposition of two successive ones, because of the lack of synchronism between camera and laser: This is the case of type F (probable superposition of C and D) and H (C and E). This reduces the number of types to six. Finally, note that the five types A–E suffice to take into account 99% of the pulses. The minimum number of types among all the series with EEs we observed is three (series 5a/29/16 has 239 EEs in a total of 29753 pulses, $d_E = 6$, and two positive Lyapunov exponents).

In the set of 64 pulses above the EE threshold, 36 correspond to type E, 23 to C, two to F, one to H, and one is missed by the camera (blind time). Now we can answer question (iii): The EEs are not associated with a single type of pattern. Yet, almost all of them are associated with only two types (E and C), and one is dominant (type E amounts to 58% of the EE). Besides, the E ones have a higher scaled average intensity (191) than the C (170, 7) and the others (171, 2). In fact, type E fills the rightmost end of the distribution in Fig. 4. There are no EEs of the A and B types although these types are, by far, the most frequent of all in the complete series.

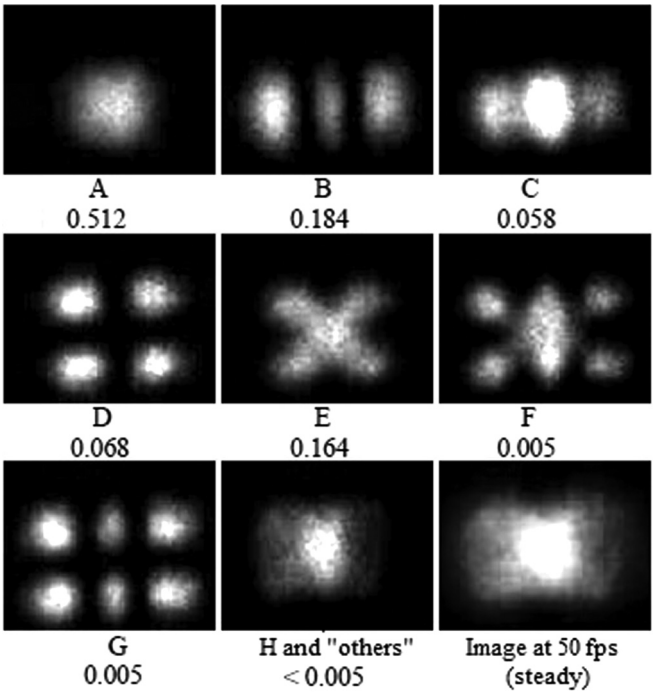

FIG. 5. Types of patterns observed in run 2b9/29/16. Their relative frequency is indicated. Probably, F = C + D and H = C + E. The spot observed with a standard camera is shown as a reference.

We can also answer question (iv): The EEs are not caused by a hot spot, but instead by a brighter illumination of the whole pattern. This pattern is *not* exclusive of the EE.

C. Sequences of patterns near an EE

Now we consider question (v), which regards the predictability of EEs. We then study their neighborhood. Since the C and E sum up to more than 90% of the total of EE, we focus on these types.

Here are a few words on notation: We indicate with a small letter the pattern corresponding to a pulse of normal intensity, and with a capital letter an EE (e.g., the sequence of patterns in Fig. 6 is *eabaEabae*). An asterisk means any pattern, and a dash means a pulse missed by the camera.

Regarding the E-type of EE, 14 (probably 15, for there is one *eab-Eabae*) out of 36 sequences are the curiously symmetrical-in-time *eabaEabae* shown in Fig. 6. A less restrictive search, seven-letter sequences, *abaEaba* increases the number only a bit, to 18. The number of sequences *eabaE***** (which are of interest to herald the EE) is 20 so that, within the set of the EE, *eaba* heralds the appearance of an E-type EE with a probability of 0.31. A striking example of the regularity of pulse intensities and time between pulses in the neighborhood of an EE is displayed in Fig. 7, where the 14 oscilloscope traces corresponding to the sequence *eabaEabae* are plotted superimposed.

Regarding the C type of EEs, and contrarily to the E type, there is no dominant sequence of nine letters. Instead, some "rare" patterns like *d, f*, and *g* appear. The sequence *adaC**** occurs 14 times, so that within the set of the EE, *ada* heralds a C-type EE with a probability of 0.22.

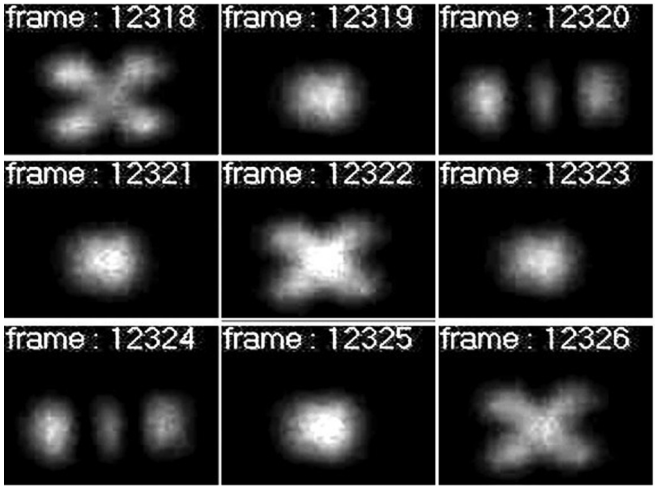

FIG. 6. An example of the sequence *eabaEabae*, which is the most frequent one in the set of EEs. It is, in addition, curiously symmetrical in time. The EE is underlined (frame 12322). See movies of this run and the one in Fig. 2 in Ref. [21].

The regularities observed reveal that the formation of EEs in this system follows a deterministic mechanism. For example, the p value corresponding to the null hypothesis that the *eabaEabae* sequence appears randomly is 3×10^{-32}. This is the result of an experiment where the probability of the appearance of this sequence in each trial is 1.1×10^{-5} (see the frequencies in Fig. 5) and there are 14 sequences in 64 trials. This extremely small p value demonstrates that this sequence is *not* the result of a statistical fluctuation.

D. Statistics on the complete series

It is interesting to know whether to predict an EE in the set of *all* the pulses in the series by using the sequence of patterns is possible, or not. In order to do this task, a computer code able to identify each type of pattern (that is, to translate each of the 27779 images into one of the eight letters in Fig. 4) is developed. The error of this code is checked by visual inspection of selected, "difficult" subsets of the series. We find

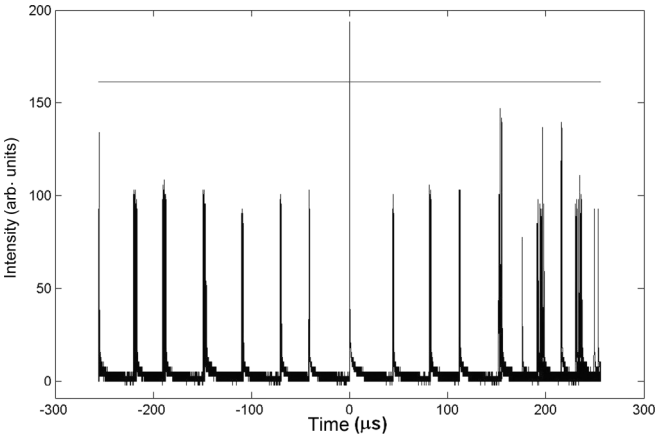

FIG. 7. Superposition of the 14 oscilloscope traces of the sequence *eabaEabae*. The horizontal line indicates the EE threshold.

that the error in recognizing a pattern strongly depends on its type. An average over all the types, weighed by their frequency, gives an error $\approx 4\%$. This number is mainly determined by the relatively high probability of erroneously identifying, as type A, some images that do not fit smoothly into one of the defined types. This code is useful whenever a pattern-recognition task is required (see the Supplemental Material [18] for the details).

Using this code, we find that the number of sequences *eabaeabae* (that is, regardless whether the *e* in the middle is an EE or not) is 321. This means that the sequence appears with a probability $\approx 1\%$ in the set of all the pulses in the series. It is far smaller than the probability within the set of EE ($15/64 \approx 23\%$). On the other hand, the probability of this sequence to happen by chance (calculated from the fractions in Fig. 5) is only $\approx 10^{-5}$. The same calculus for the *adac* sequence (which is the other most common sequence leading to EE) shows that it has a probability to happen by chance of $\approx 10^{-3}$, but there are 328 of these sequences in the complete series ($>1\%$), and $14/69 \approx 20\%$ within the set of the EEs. In other words, the sequences *eabaeabae* and *adac* appear, in the complete series, far more often (a factor of 10–1000) than randomly. They do it even more often (an additional factor of 20) within the set of EEs. These results indicate that the system follows some preferred "roads" of patterns in its evolution, and that at least two of these roads are likely to produce an EE. These are encouraging results. The identification of these roads (actually, sets of orbits within the attractor) is the first step to achieve EE management through control of chaos.

However, despite the regularities found, the probability of predicting an EE from a sequence of patterns is poor. The number of sequences *eaba* is 2173, but only 15 EEs (all of type E) follow. The number of sequences *ada* is 1369, but only 14 EEs (all of type C) follow. Therefore, the sequence of patterns does not provide a reliable way to herald an EE. The number of "false alarms" is too high.

Finally, note that practically all EEs belong to the types C, E, or F. These types also reach higher average energies than the other ones by a factor of 1.5–2 (see the Supplemental Material [18]). This result can be understood by noting that the images in Fig. 5 show that these types overlap the transverse pumped area best. It is then possible to hypothesize the basic mechanism of formation of EEs in this way: The patterns with EEs have the spatial distributions most efficient to extract energy from the pumped area and, *in addition*, for some reason still to be fully explained, sometimes do it extraordinarily well. The reason for this success surely lies in the spatial distribution of the bleaching of the SA. In Ref. [16] it was shown that EEs are *not* preceded by a long time elapsed since the last pulse; that is, they are not caused by the simple accumulation of energy because of a longer pump time. Recall also that Cr:YAG is a slow SA, so that it keeps some memory of the bleaching level reached in the previous pulse.

IV. CONCLUSIONS

One of the goals of our research program is to manage the formation of EEs for a practical application. This requires the development of an appropriate (not only correct, but also as simple as possible) mathematical description of the phenomenon. It is useful summarizing here the observations

that description must fit. In previous contributions [11,16] we have reported the following:

(1) Chaotic regimes have been observed with all values of $d_E \geqslant 4$, but no regime with EEs has been observed with $d_E < 6$. EEs are easier to observe with increasing Fresnel number. EEs are observed in regimes with one or more positive Lyapunov exponents as well.

(2) The regimes with EEs show a decay of the correlation between the time series recorded at different points in the transverse section. The chaotic regimes without EEs do not always show this decay. The same happens with the transverse phase coherence observed in a Mach-Zehnder interferometer. These results indicate that a description in terms of *intensities* (instead of *fields*) may suffice [22].

(3) The time before the appearance of an EE (measured since the previous pulse) is well defined and near the average time between successive pulses. On the contrary, the time after an EE until the next pulse is longer than the average (which is most reasonable).

In this paper, we add the following:

(4) It suffices to take into account the interaction within a set of relatively few modes that are previously determined by the observation. The time series analyzed in this paper need five patterns to take into account 99% of the pulses. Similar numbers are obtained in other recorded series, but are not analyzed here. This means that the mathematical description does not need to include the transversal Laplacian, but a set of relatively few ordinary differential equations, which significantly simplifies the problem.

(5) The patterns associated with EEs seem to be the most efficient to extract energy from the active medium, because of their overlap with the pumped area.

(6) The pulse separation and intensity, as well as the sequence of patterns, just before and after an EE, are more regular than for a non-EE pulse.

The observed regularities indicate that the EEs occur inside a well defined set of orbits. The formation of EEs can be then managed by stabilizing these orbits through algorithms of control of chaos. Besides, that region of phase space is visited much more often than in a random evolution, what is a fortunate feature regarding the foreseen practical application, for the user does not have to wait a long time (at the human time scale) until an opportunity to generate an EE spontaneously arises.

The next step in our program is the development of a mathematical description. As it is said, simplicity is crucial to devising a control algorithm to be feasible in practice. From the observations summarized above, we know the description can be based on a few intensity modes, coupled through the populations in the gain and the SA. The theoretical results should be then checked against those observations. If a poor fitting is obtained, we foresee several steps of increasing complexity of the description. In the simplest approach, no spatial modulations of the population in the SA are taken into account, as in [22]. The next step is to include these spatial modulations, but with a fixed phase relationship. A third possible step is to consider the phases as free variables.

The observations reported in this paper reveal that the complex steady transverse pattern observed with a standard camera is the superposition of a few simpler patterns that alternate chaotically, that the patterns corresponding to EEs belong to an even smaller set, and that the sequences of patterns before (and sometimes after) an EE are repetitive. Besides, all the simple patterns are free of hot spots and are similar to low order modes of the optical cavity. This information is obtained thanks to the use of an ultrafast camera and two programs specifically developed to analyze the data.

There is no reason to believe these results to be specific of solid-state lasers. On the contrary, they should be *prima facie* valid in other types of lasers+SA with transversally extended cavities, where the dynamics is too fast to allow direct observation of the spatial pattern associated with each pulse (as in [12,13]). These results can be hence taken as the starting hypothesis in any high Fresnel number laser+SA system. Even more generally, these results demonstrate that EEs can arise even in a system with a limited number of modes. Hence, an equation in partial derivatives (as the often used nonlinear Schrödinger equation) is not necessarily involved in the formation of EEs.

ACKNOWLEDGMENTS

Many, many thanks to Professor P. Mininni and Professor P. Cobelli, Laboratorio de Turbulencia Geofísica, Facultad de Ciencias Exactas y Naturales, Universidad de Buenos Aires, for lending us the ultrafast camera, and to Dr. R. Espada, Departamento de Química Biológica, in the same institution, for advice and help in developing the pattern-recognition code. This material is based upon work supported by the Air Force Office of Scientific Research (USA) under Award No. FA9550-16-C-0045, "Nonlinear dynamics of self-pulsing all-solid-state lasers". It also received support from the CONICET (Argentina), Grant No. PIP2011-077 "Desarrollo de láseres sólidos bombeados por diodos y de algunas de sus aplicaciones", and ECOS-Sud (France-Argentina) Project No. A14E03, "Extreme Events in Nonlinear systems".

[1] C. Kharif, E. Pelinovsky, and A. Slunyaev, *Rogue Waves in the Ocean* (Springer-Verlag, Berlin, Heidelberg, 2009).

[2] D. Solli, C. Ropers, P. Koonath, and B. Jalali, Optical extreme events, Nature **450**, 1054 (2007).

[3] C. Finot, K. Hammami, J. Fatome, J. Dudley, and G. Millot, Selection of extreme events generated in Raman fiber amplifiers through spectral offset filtering, IEEE J. Quantum Electron. **46**, 205 (2010).

[4] A. Montina, U. Bortolozzo, S. Residori, and F. T. Arecchi, Non-Gaussian Statistics and Extreme Waves in a Nonlinear Optical Cavity, Phys. Rev. Lett. **103**, 173901 (2009).

[5] C. Bonatto, M. Feyereisen, S. Barland, M. Giudici, C. Masoller, J. Ríos Leite, and J. Tredicce, Deterministic Optical Extreme Events, Phys. Rev. Lett. **107**, 053901 (2011).

[6] J. Soto-Crespo, P. Grelu, and N. Akhmediev, Dissipative rogue waves: Extreme pulses generated by passively mode-locked lasers, Phys. Rev. E **84**, 016604 (2011).

[7] A. Zaviyalov, O. Egorov, R. Iliew, and F. Lederer, Rogue waves in mode-locked fiber lasers, Phys. Rev. A **85**, 013828 (2012).

[8] C. Lecaplain, P. Grelu, J. Soto-Crespo, and N. Akhmediev, Dissipative Rogue Waves Generated by Chaotic Pulse Bunching in a Mode-Locked Laser, Phys. Rev. Lett. **108**, 233901 (2012).

[9] A. Runge, C. Aguergaray, N. Broderick, and M. Erkintalo, Raman rogue waves in a partially mode-locked fiber laser, Opt. Lett. **39**, 319 (2014).

[10] M. Kovalsky, A. Hnilo, and J. Tredicce, Extreme events in the Ti:sapphire laser, Opt. Lett. **36**, 4449 (2011).

[11] C. Bonazzola, A. Hnilo, M. Kovalsky, and J. Tredicce, Optical rogue waves in the all-solid-state laser with a saturable absorber: importance of the spatial effects, J. Opt. **15**, 064004 (2013).

[12] F. Selmi, S. Coulibaly, Z. Loghmari, I. Sagnes, G. Beaudoin, M. G. Clerc, and S. Barbay, Spatiotemporal Chaos Induces Extreme Events in an Extended Microcavity Laser, Phys. Rev. Lett. **116**, 013901 (2016).

[13] S. Coulibaly, M. G. Clerc, F. Selmi, and S. Barbay, Extreme events following bifurcation to spatiotemporal chaos in a spatially extended microcavity laser, Phys. Rev. A **95**, 023816 (2017).

[14] J. Dudley, F. Dias, M. Erkintalo, and G. Genty, Instabilities, breathers and rogue waves in Optics, Nat. Photonics **8**, 755 (2014).

[15] C. Rimoldi, S. Barland, F. Prati, and G. Tissoni, Spatiotemporal extreme events in a laser with a saturable absorber, Phys. Rev. A **95**, 023841 (2017).

[16] C. R. Bonazzola, A. A. Hnilo, M. G. Kovalsky, and J. R. Tredicce, Features of the extreme events observed in an all-solid-state laser with a saturable absorber, Phys. Rev. A **92**, 053816 (2015).

[17] J. Flood, D. Walker, and H. van Driel, Effect of spatial hole burning in a mode-locked diode end-pumped Nd:YAG laser, Opt. Lett. **20**, 58 (1995).

[18] See Supplemental Material at http://link.aps.org/supplemental/10.1103/PhysRevE.97.032215 for the description of the computer codes and for histograms of the energy distributions of each type of pattern.

[19] R. Hegger, H. Kantz, and T. Schreiber, Practical implementation of nonlinear time series methods: The TISEAN package, Chaos **9**, 413 (1999).

[20] T. Schreiber and A. Schmitz, Surrogate time series, Phys. D (Amsterdam, Neth.) **142**, 346 (2000).

[21] See http://www.lls-ceilap.com/extreme-events-in-all-solid-state-lasers.ht.

[22] J. Dong, K.-I Ueda, and P. Yang, Multi-pulse oscillation and instabilities in microchip self-Q-switched transverse-mode laser, Opt. Express **17**, 16980 (2009).